

## Canted antiferromagnetism in an insulating lightly doped $\text{La}_{1-x}\text{Sr}_x\text{MnO}_3$ with $x \leq 0.17$

H. Kawano

*Institute of Physical and Chemical Research, Wako, Saitama 351-01, Japan*

R. Kajimoto, M. Kubota, and H. Yoshizawa

*Neutron Scattering Laboratory, Institute for Solid State Physics, University of Tokyo, Shirakata 106-1, Tokai, Ibaraki 319-11, Japan*

(Received 7 September 1995; revised manuscript received 18 October 1995)

We have investigated the magnetic structure of an insulating lightly doped  $\text{La}_{1-x}\text{Sr}_x\text{MnO}_3$  with  $x=0.04, 0.125$ , and  $0.17$  with neutron scattering technique and bulk magnetization measurements. The magnetic structure of the  $x=0.04$  sample at 5 K is a commensurate layer-type (A-type) antiferromagnetism with the propagation vector  $[010]$  and the moment of  $3.7 \pm 0.2 \mu_B/\text{Mn}$ , being parallel to the  $[100]$  axis in the orthorhombic  $Pnma$  symmetry. In addition, a spontaneous magnetization of  $0.28 \pm 0.02 \mu_B/\text{Mn}$  is observed at 8 K by magnetization measurement. By contrast, the  $x=0.125$  sample exhibits a large ferromagnetic moment of  $3.7 \pm 0.2 \mu_B/\text{Mn}$  and a small A-type antiferromagnetic component of  $0.23 \pm 0.1 \mu_B/\text{Mn}$ , while the  $x=0.17$  sample exhibits only a ferromagnetic component of  $3.6 \pm 0.2 \mu_B/\text{Mn}$ . These results are consistent with a spin structure derived from the conventional double exchange mechanism, but rule out the possibility of a recently suggested spiral spin structure for the insulating  $\text{La}_{1-x}\text{Sr}_x\text{MnO}_3$  system.

Distorted perovskite manganese oxides such as  $\text{La}_{1-x}\text{Sr}_x\text{MnO}_3$  and  $\text{La}_{1-x}\text{Ca}_x\text{MnO}_3$  transform from an antiferromagnetic insulator to a ferromagnetic metal as substitution of La ions by alkaline-earth ions.<sup>1-4</sup> Such behavior has been long known as metallic transport phenomena mediated by a double exchange mechanism.<sup>5-7</sup> The recent discovery of a gigantic magnetoresistance,<sup>8-15</sup> lattice-structure switching by an external field<sup>16</sup> as well as field-induced insulator-metal transitions<sup>17-19</sup> has renewed interest in these perovskite-type manganese oxide systems. Manganese ions in the parent material  $\text{LaMnO}_3$  have a  $3d^4$  configuration where three electrons occupy the  $t_{2g}$  orbitals, while one electron occupies the  $e_g$  orbital. The number of  $e_g$  electrons in  $\text{LaMnO}_3$  corresponds to half filling, and makes the parent  $\text{LaMnO}_3$  a Mott-type antiferromagnetic insulator. The substitution of La ions by divalent ions leads to doping of holes to the  $e_g$  orbitals, introducing an itinerant character as well as ferromagnetism to well-doped samples. For a lightly doped insulating regime of the solid solution system  $\text{La}_{1-x}\text{Sr}_x\text{MnO}_3$ , however, the double exchange model suggests a canted antiferromagnetism as the magnetic structure.<sup>7</sup> On the other hand, based on a mean field treatment of localized  $t_{2g}$  electrons and itinerant  $e_g$  electrons with a strong Hund coupling, Inoue and Maekawa<sup>20</sup> recently proposed that a spiral state can be energetically more favorable than a canted antiferromagnetic state for a nearly half-doped insulating regime. This theory suggests that the spiral state continuously changes to the ferromagnetic state as a function of hole doping from half filling.

In a pioneering work by Wollan and Koehler in 1955, the magnetic structures of the  $\text{LaMnO}_{3+\delta}$  system as well as the  $\text{La}_{1-x}\text{Ca}_x\text{MnO}_3$  system were studied by the neutron diffraction technique.<sup>2</sup> The spin structure of the  $\text{LaMnO}_{3+\delta}$  system was reported to be a canted antiferromagnet where a layer type (a so-called A-type) antiferromagnetic (AF) structure coexists with a ferromagnetic (F) moment as shown in Fig. 1. The AF moment was found to lie in the  $Pnma$   $ac$  plane,

but its precise direction was not determined. It was found that the off-stoichiometry of oxygen  $\delta$  progressively enhances the spontaneous F moment. The magnetic structure of the doped system  $\text{La}_{1-x}\text{Ca}_x\text{MnO}_3$  was also studied, and the magnetic phase diagram of the  $\text{Mn}^{4+}$  ion concentration  $y$  versus temperature was reported, where the coexistence of F and AF moments was found for the  $\text{Mn}^{4+}$  ion concentration of  $0.1 < y < 0.25$ . The  $\text{LaMnO}_{3+\delta}$  and  $\text{La}_{1-x}\text{Ca}_x\text{MnO}_3$  systems were further studied by Matsumoto in 1970.<sup>4</sup> Through the examination of the  $\text{LaMnO}_{3+\delta}$  system, he established that a weak ferromagnetism is intrinsic to stoichiometric  $\text{LaMnO}_3$ .

From the measurements of resistivity and magnetization, the Sr concentration versus temperature phase diagram for the  $\text{La}_{1-x}\text{Sr}_x\text{MnO}_3$  system was reported recently by Urushibara *et al.*, where the insulating phase is located for  $x < 0.175$ .<sup>15</sup> Following the early work on the  $\text{La}_{1-x}\text{Ca}_x\text{MnO}_3$  system,<sup>2</sup> the low-temperature phase is as-

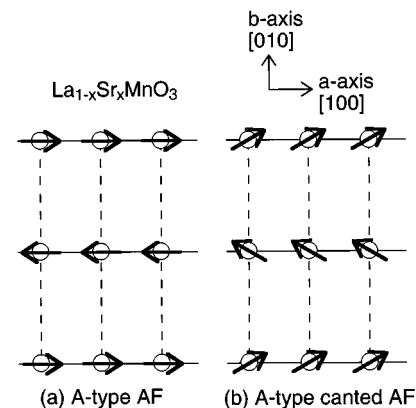


FIG. 1. Schematic illustration of a layer-type antiferromagnetic structure. This structure is labeled as A-type after Wollan and Koehler (Ref. 2).

signed to the canted AF phase for  $x \leq 0.1$ , and to the insulating F phase for  $0.1 < x < 0.175$ . To our knowledge, however, there is no neutron diffraction study on the magnetic structure in an insulating  $\text{La}_{1-x}\text{Sr}_x\text{MnO}_3$  system, although the ferromagnetic metallic sample with  $x=0.3$  has been studied very recently.<sup>21</sup> Consequently, we have studied the magnetic structure of insulating lightly doped  $\text{La}_{1-x}\text{Sr}_x\text{MnO}_3$  samples with  $x=0.04, 0.125$ , and  $0.17$  by the neutron scattering technique as well as magnetization measurements in order to examine the possible existence of a spiral state. For three samples we have also found an interesting variation of the lattice structure as a function of temperature and hole doping, and such results will be reported separately.<sup>22</sup>

Polycrystalline samples were prepared by powdering melt-grown samples. First, a prescribed amount of dried powder of  $\text{La}_2\text{O}_3$ ,  $\text{SrCO}_3$  and  $\text{Mn}_2\text{O}_3$  was well mixed in ethanol and dried, and then fired at  $1000^\circ\text{C}$  in air for 6 h. The precalcined powder was pressed into rods with a hydrostatic pressure of  $1.4 \text{ ton/cm}^2$ , and fired again at  $1100^\circ\text{C}$  in air for 38 h. Second, the single-crystal samples were melt grown with the floating zone method. A prepared rod was loaded to a floating zone furnace with a flow of Ar gas of  $400 \text{ cm}^3/\text{min}$  and traveled at  $2 \text{ mm/h}$ . Finally, the single-crystal samples were powdered. Measurements of x-ray powder diffraction showed that the obtained materials were of single phase. For the three samples studied, all magnetic as well as structural transition temperatures were consistent with the reported values in Ref. 15.

Neutron diffraction measurements were performed with the triple-axis spectrometers GPTAS and HER at the JRR-3M in JAERI, Tokai. The spectrometers were operated with their double-axis mode, and the (002) reflection of pyrolytic graphite composite monochromators was utilized to obtain incident neutron momentum of  $k_i = 2.67 \text{ \AA}^{-1}$  at GPTAS and  $k_i = 1.55 \text{ \AA}^{-1}$  at HER, respectively. For the GPTAS experiments, collimators of  $40' - 20' - 20'$  were placed at three positions from inpile to monochromator, between monochromator and sample, and between sample to detector, while for the HER experiments,  $40'$  collimators were placed before and after sample, respectively. Samples were set into an aluminum capsule, and it was placed in a closed cycle helium gas refrigerator, and the sample temperature ranging from 10 K to 350 K was controlled within accuracy of  $0.1^\circ$ .

Magnetization measurements were performed with the use of a conventional superconducting quantum interference device (SQUID) magnetometer. The sample was cooled in a field of 0.01 T from the paramagnetic phase, and then the temperature dependence of the magnetization ( $M$ ) was recorded with rising temperature. The measurements were carried out in a field of 0.01 T in order to minimize a rounding of the ferromagnetic transition due to an applied field.

Figure 2 shows part of the powder patterns for three samples with  $x=0.04, 0.125$ , and  $0.17$ . The antiferromagnetic (010) Bragg reflection is shown in the left column, while nuclear as well as ferromagnetic (101) and (020) reflections are shown in the right column, respectively. We first describe the results of the  $\text{La}_{0.96}\text{Sr}_{0.04}\text{MnO}_3$  sample. Powder patterns were observed at 200 K and 10 K. Standard Rietvelt analyses<sup>23</sup> showed that the crystal of the  $\text{La}_{0.96}\text{Sr}_{0.04}\text{MnO}_3$  sample belongs to the space group  $Pnma$  with lattice con-

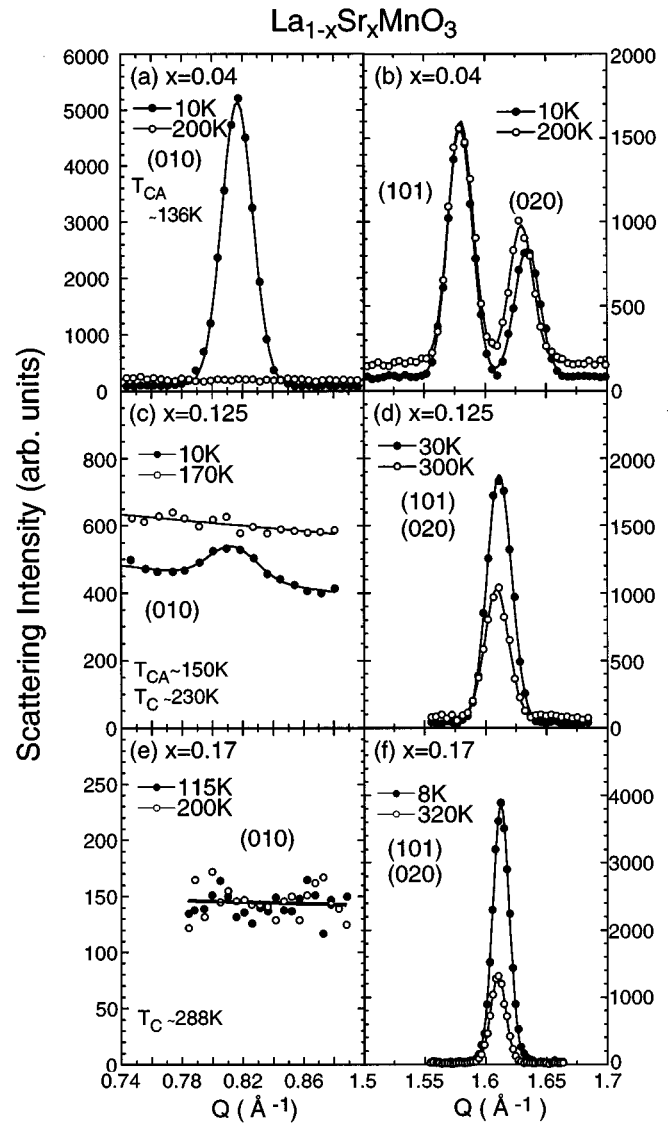


FIG. 2. Selected portion of powder patterns for the  $x=0.04, 0.125$ , and  $0.17$  samples. Panels (a), (c), and (e) give the observed scattering patterns near the magnetic (010) Bragg reflection, while those of (b), (d), and (f) illustrate the profiles of the orthorhombic (101) and (020) Bragg reflections, respectively. Note that, in panel (f), (012) is the correct index for the rhombohedral symmetry at 320 K.

stants  $a = 5.697(1) \text{ \AA}$ ,  $b = 7.709(2) \text{ \AA}$ , and  $c = 5.547(1) \text{ \AA}$  at 200 K, and  $a = 5.701(1) \text{ \AA}$ ,  $b = 7.687(2) \text{ \AA}$ , and  $c = 5.550(1) \text{ \AA}$  at 10 K, respectively. These lattice constants satisfy the relation  $b/\sqrt{2} < c < a$  for a so-called  $O'$  orthorhombic structure, indicating that the lattice distortion is caused by the Jahn-Teller effect of  $\text{Mn}^{3+}$  ions.<sup>24</sup> Only nuclear Bragg reflections were observed in the paramagnetic phase at 200 K, while magnetic superlattice reflections appeared at 10 K, e.g., the (010) AF Bragg reflection shown in Fig. 2(a). From the reflection condition and intensity analysis, we have found that the magnetic structure in the  $x=0.04$  sample is an A-type AF structure as shown in Fig. 1, and the ordered moment is determined to be  $3.7 \mu_B \pm 0.2 \mu_B/\text{Mn}$ , being parallel to the  $[100]$  axis. In early

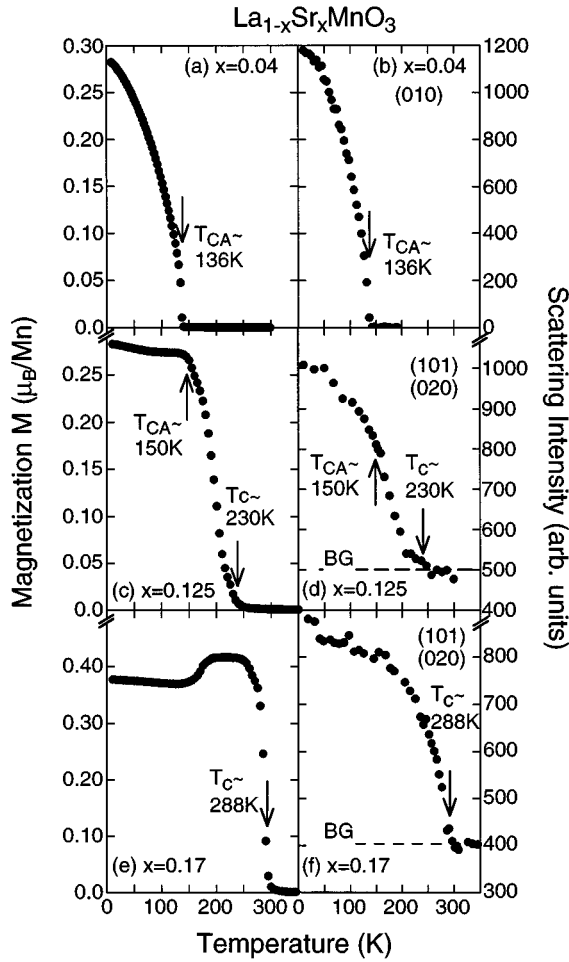


FIG. 3. Left column: temperature dependences of field cooled magnetization observed at  $H=0.01$  T for  $x=0.04$ ,  $0.125$ , and  $0.17$  samples. Right column: temperature dependences of the integrated intensity observed at  $Q=(010)$  for  $x=0.04$ , and at  $Q=(101)$  and  $(020)$  for  $x=0.125$  and  $0.17$  samples, respectively.

neutron work,<sup>2</sup> the AF moment in the  $\text{LaMnO}_3$  sample was reported to lie in the  $ac$  plane, whereas in the present study, we have found that it is parallel to the  $[100]$  axis. It should be noted that Matsumoto predicted the  $[100]$  axis as the moment direction from consideration of the spin Hamiltonian formalism.<sup>4</sup>

To examine the ferromagnetic (F) component, the temperature dependence of the magnetization ( $M$ ) of the  $x=0.04$  sample was measured and is shown in Fig. 3(a). A spontaneous magnetization appears at  $T_{CA} \sim 136$  K and increases monotonically below  $T_{CA}$  with decreasing temperature. This indicates the existence of the ferromagnetic component below  $T_{CA}$ . The spontaneous magnetization at 8 K was determined to be  $0.28 \pm 0.02 \mu_B/\text{Mn}$ . The temperature dependence of the AF component is shown in Fig. 3(b). Combining the results of magnetization measurements and neutron diffraction experiments, we have found that the AF and F long-range orders take place at the same temperature  $T_{CA} \sim 136$  K in the  $\text{La}_{0.96}\text{Sr}_{0.04}\text{MnO}_3$  sample. Namely, the magnetic structure of the  $\text{La}_{0.96}\text{Sr}_{0.04}\text{MnO}_3$  sample is a canted-layer-type ( $A$ -type) antiferromagnetic order with propagation vector  $[010]$  and an ordered moment of  $3.7 \pm 0.2 \mu_B/\text{Mn}$ .

Returning to Fig. 2, the profiles of the AF and F Bragg peaks in the  $x=0.125$  sample are illustrated in the middle panels Figs. 2(c) and 2(d). A weak AF Bragg reflection was observed at  $(010)$ . The increase of intensity at 170 K is due to the paramagnetic scattering of Mn moments. A similar increase of the background intensity in the paramagnetic phase is also seen in Figs. 2(a), 2(b), and 2(d). The moment of the AF component was determined to be  $0.23 \pm 0.1 \mu_B/\text{Mn}$  at 10 K. In Fig. 2(d) is shown the profiles of the  $(101)$  and  $(020)$  Bragg reflections. Compared with the corresponding Bragg peaks for the  $x=0.04$  sample shown in Fig. 2(b), the  $(101)$  and  $(020)$  reflections for the  $x=0.125$  sample appear at almost the same scattering vector. The increase at 30 K is due to the F component with a moment of  $3.7 \pm 0.2 \mu_B/\text{Mn}$ . From the temperature dependence of the F component as well as that of the magnetization shown in Figs. 3(c) and 3(d), we have found that the  $x=0.125$  sample orders ferromagnetically at  $T_C \sim 230$  K, but transforms to a canted  $A$ -type AF structure below  $T_{CA} \sim 150$  K. To determine  $T_{CA}$ , the temperature dependence of the AF component was measured with the use of a single-crystal sample. Finally, the profiles of the  $x=0.17$  sample are shown in panels Figs. 2(e) and 2(f). No AF Bragg peak was observed within the accuracy of scatter of the data. By contrast, a clear intense F component of  $3.6 \pm 0.2 \mu_B/\text{Mn}$  is seen at the  $(101)$  and  $(020)$  positions. The Curie temperature of the  $x=0.17$  sample is determined to be  $T_C \sim 288$  K from the temperature dependence of the magnetization and that of the profiles of  $(101)$  and  $(020)$  shown in Figs. 3(e) and 3(f), from which one can clearly see the onset of the F long-range order at  $T_C \sim 288$  K. The decrease of the magnetization at  $T \approx 170$  K is correlated with the structural transition from rhombohedral symmetry to orthorhombic  $Pnma$ .<sup>15,22</sup>

The concentration dependence of the magnetic structure is summarized in Fig. 4. The upper panel shows the concentration dependence of the moment of the AF and F components, while the lower panel gives that of the position in momentum space. The dominant component crosses over from the AF component to the F component at around  $x \sim 0.08$  in the  $\text{La}_{1-x}\text{Sr}_x\text{MnO}_3$  system. A similar crossover was observed near  $x \sim 0.15$  in the  $\text{La}_{1-x}\text{Ca}_x\text{MnO}_3$  system in the early study.<sup>2</sup> From the lower panel, one can see that the positions of the magnetic Bragg reflections are locked at either the AF position  $(0, \pi, 0)$  or the F position  $(0, 0, 0)$ . If the spin structure continuously varies from  $(0, \pi, 0)$  to  $(0, 0, 0)$  through a spiral spin arrangement due to hole doping, the locus of the peak position should follow the dashed line in the panel, and this argument holds for a fan-type spin structure as well.

It is interesting to point out that there is a rather sharp changeover of the AF and F components in the  $\text{La}_{1-x}\text{Sr}_x\text{MnO}_3$  system despite a linear variation of the hole density over the interested insulating region of the Sr concentration, and this changeover takes place at  $x \sim 0.08$  which is almost half the corresponding dopant concentration in the  $\text{La}_{1-x}\text{Ca}_x\text{MnO}_3$  system. Recently, a phase diagram of the temperature versus tolerance factor for the closely related system with a fixed hole concentration was reported,<sup>25</sup> from which one can see that the ferromagnetic metal-insulator transition boundary is very much sensitive to the cation size through the tolerance factor. A larger cation, and therefore a larger tolerance factor, favors the metallic phase for the fixed

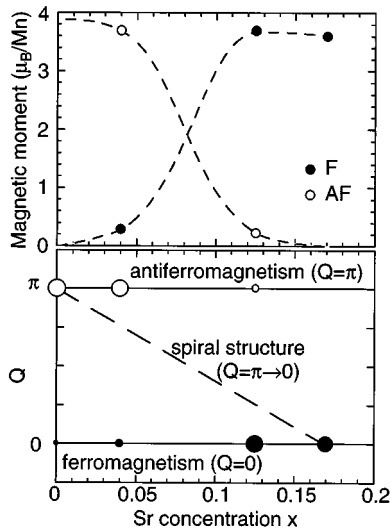


FIG. 4. Upper panel: Sr concentration dependence of the F and AF components. Lower panel: Sr concentration dependence of the Bragg peak positions for the AF and F components.

hole concentration. Since the radius of  $\text{Sr}^{2+}$  ions is larger than that of  $\text{Ca}^{2+}$  ions, the insulator-metal transition in the  $\text{La}_{1-x}\text{Sr}_x\text{MnO}_3$  system takes place at a smaller hole concentration than that in the  $\text{La}_{1-x}\text{Ca}_x\text{MnO}_3$  system. Consequently, it is plausible that the AF to F changeover also takes

place at smaller dopant ion concentration in the  $\text{La}_{1-x}\text{Sr}_x\text{MnO}_3$  system.

In summary, we have studied the magnetic behavior of  $\text{La}_{1-x}\text{Sr}_x\text{MnO}_3$  samples with  $x=0.04, 0.125,$  and  $0.17$ . In  $\text{La}_{0.96}\text{Sr}_{0.04}\text{MnO}_3$ , magnetic Bragg reflections are observed below  $T_{CA} \sim 136$  K. The magnetic structure determined is a commensurate layer-type (A-type) antiferromagnetism with the propagation vector  $[010]$  and the moment of  $3.7 \pm 0.2 \mu_B/\text{Mn}$  at 5 K, being parallel to the  $[100]$  axis. In addition, a spontaneous magnetization of  $0.28 \pm 0.02 \mu_B/\text{Mn}$  is observed at 8 K by magnetization measurements. The  $\text{La}_{0.875}\text{Sr}_{0.125}\text{MnO}_3$  sample orders ferromagnetically at  $T_C \sim 230$  K, but accompanies a canted A-type AF order below  $T_{CA} \sim 150$  K, and exhibits a large F moment of  $3.7 \pm 0.2 \mu_B/\text{Mn}$  as well as an A-type AF moment of  $0.23 \pm 0.1 \mu_B/\text{Mn}$  at 10 K. For the  $\text{La}_{0.83}\text{Sr}_{0.17}\text{MnO}_3$  sample, it orders ferromagnetically at  $T_C \sim 288$  K, and shows a F moment of  $3.6 \pm 0.2 \mu_B/\text{Mn}$  at 8 K, but no AF Bragg reflection within accuracy of the data. Combining these results, we conclude that the magnetic ordering of an insulating lightly doped  $\text{La}_{1-x}\text{Sr}_x\text{MnO}_3$  with  $x < 0.17$  is a canted antiferromagnetism rather than a spiral order.

One of the authors (H.K.) would like to thank Dr. K. Katsumata for helpful advice and valuable discussions, and for use of a SQUID magnetometer. This work was supported by Special Researcher's Basic Science Program (RIKEN) and by a Grant-In-Aid for Scientific Research from the Ministry of Education, Science and Culture, Japan.

- <sup>1</sup>G.H. Jonker and J.H. van Santen, *Physica* **16**, 337 (1950).
- <sup>2</sup>E.O. Wollan and W.C. Koehler, *Phys. Rev.* **100**, 545 (1955).
- <sup>3</sup>G.H. Jonker, *Physica* **22**, 707 (1956).
- <sup>4</sup>G. Matsumoto, *J. Phys. Soc. Jpn.* **29**, 606 (1970); **29**, 615 (1970).
- <sup>5</sup>C. Zener, *Phys. Rev.* **82**, 403 (1951).
- <sup>6</sup>P.W. Anderson and H. Hasegawa, *Phys. Rev.* **100**, 675 (1955).
- <sup>7</sup>P.-G. de Gennes, *Phys. Rev.* **118**, 141 (1960).
- <sup>8</sup>R.M. Kusters, D.A. Singleton, D.A. Keen, R. McFreevy, and W. Hayes, *Physica B* **155**, 362 (1989).
- <sup>9</sup>K. Chabara, T. Ohno, M. Kasai, and Y. Kozono, *Appl. Phys. Lett.* **63**, 1990 (1993).
- <sup>10</sup>R. von Helmont, J. Wecker, B. Holzapfel, L. Schultz, and K. Samwer, *Phys. Rev. Lett.* **71**, 2331 (1993).
- <sup>11</sup>S. Jin, Th.H. Tiefel, M. McCormack, R.A. Fastnacht, R. Ramesh, and L.H. Chen, *Science* **264**, 413 (1994).
- <sup>12</sup>H.L. Ju, C. Kwon, R.L. Greene, and T. Venkatesan, *Appl. Phys. Lett.* **65**, 2108 (1994).
- <sup>13</sup>M. McCormack, S. Jin, T.H. Tiefel, R.M. Fleming, and Julia W. Phillips, *Appl. Phys. Lett.* **64**, 3045 (1994).
- <sup>14</sup>Y. Tokura, A. Urushibara, Y. Moritomo, T. Arima, A. Asamitsu, G. Kido, and N. Furukawa, *J. Phys. Soc. Jpn.* **63**, 3931 (1994).
- <sup>15</sup>A. Urushibara, Y. Moritomo, T. Arima, A. Asamitsu, G. Kido, and Y. Tokura, *Phys. Rev. B* **51**, 14 103 (1995).
- <sup>16</sup>A. Asamitsu, Y. Moritomo, Y. Tomioka, T. Arima, and Y. Tokura, *Nature (London)* **373**, 407 (1995).
- <sup>17</sup>Y. Tomioka, A. Asamitsu, Y. Moritomo, H. Kuwahara, and Y. Tokura, *Phys. Rev. Lett.* **74**, 5108 (1995).
- <sup>18</sup>Y. Tomioka, A. Asamitsu, H. Kuwahara, Y. Moritomo, and Y. Tokura, *J. Phys. Soc. Jpn.* **64**, 3626 (1995).
- <sup>19</sup>H. Yoshizawa, H. Kawano, Y. Tomioka, and Y. Tokura, *Phys. Rev. B* **51**, R13 145 (1995).
- <sup>20</sup>J. Inoue and S. Maekawa, *Phys. Rev. Lett.* **74**, 3407 (1995).
- <sup>21</sup>M.C. Martin, G. Shirane, Y. Endoh, K. Hirota, Y. Moritomo, and Y. Tokura (unpublished).
- <sup>22</sup>H. Kawano, R. Kajimoto, M. Kubota, and H. Yoshizawa (unpublished).
- <sup>23</sup>F. Izumi, in *The Rietveld Method*, edited by R.A. Young (Oxford University Press, Oxford, 1993), Chap. 13; Y.-I. Kim and F. Izumi, *J. Ceram. Soc. Jpn.* **102**, 401 (1994).
- <sup>24</sup>J.B. Goodenough, A. Wold, R.J. Arnett, and N. Menyuk, *Phys. Rev.* **124**, 373 (1961).
- <sup>25</sup>H.Y. Hwang, S-W. Cheong, P.G. Radaelli, M. Marezio, and B. Batlogg, *Phys. Rev. Lett.* **75**, 914 (1995).